



Brain Function and Structure Changes in the Prognosis Prediction of Prolonged Disorders of Consciousness

Weiguan Chen⁴ · Ye Zhang² · Aisong Guo¹ · Xuejun Zhou³ · Weiqun Song²

Received: 17 November 2022 / Accepted: 20 October 2024

© The Author(s), under exclusive licence to Springer Science+Business Media, LLC, part of Springer Nature 2024

Abstract

Objectives To observe the functional differences in the key brain areas in patients with different levels of consciousness after severe brain injury, and provide reference for confirming the objective diagnosis indicators for prolonged disorders of consciousness (pDoCs).

Methods This prospective study enrolled patients with pDoCs hospitalized in the department of rehabilitation medicine of our Hospital. Levels of consciousness and clinical outcomes were assessed according to diagnostic criteria and behavioral scales. Resting-state functional magnetic resonance imaging (rs-fMRI) and diffusion tensor imaging (DTI) of 30 patients with different levels of consciousness was performed. The patients were grouped as conscious or unconscious according to whether they regained consciousness during the 12-month follow-up.

Results Thirty patients were enrolled, including eight with unresponsive wakefulness syndrome/vegetative state, eight with minimally conscious state, six with emergence from the minimally conscious state, and eight with a locked-in syndrome. There were 19 and 11 patients in the conscious and unconscious groups. Compared with the unconscious group, the left basal nucleus was activated in the conscious group, and there were significant differences in white matter fiber bundles. Correlations were observed between the regional homogeneity (ReHo) value of the cerebellum and the Glasgow coma scale score ($r = 0.387$, $P = 0.038$) and between the ReHo value of the left temporal and the coma recovery scale-revised score ($r = 0.394$, $P = 0.035$).

Conclusions The left insula and cerebellum might be important for regaining consciousness. The brain function activity and structural remodeling of the key brain regions and the activation level of the cerebellum are correlated with clinical behaviors and have potential application value for the prognosis prediction of pDoCs patients.

Keywords Disorders of Consciousness · Functional Magnetic Resonance Imaging · Diffusion Tensor Imaging · Brain Network · Prognosis

Introduction

Severe brain injury (SBI) is a structural injury and/or physiologic disruption of brain function resulting from trauma, ischemia (e.g., stroke and hypoxic-ischemic encephalopathy (HIE), hemorrhage, neuronal damage (e.g., infections), or structural disruptions (e.g., tumors) and leading to new onset of any period of confusion, disorientation, change in consciousness, or amnesia that may or may not be transient (does not require loss of consciousness), observed neurologic dysfunction, and intracranial lesion (Powers et al. 2019). Any of the following characterizes a moderate-to-severe brain injury: abnormal cerebral imaging, loss of consciousness > 30 min, altered mental status > 24 h, post-traumatic amnesia > 1 day, and best Glasgow Coma Scale

Communicated by Christoph Michel.

✉ Weiqun Song
songwq66@126.com

¹ Department of Rehabilitation Medicine, Affiliated Hospital of Nantong University, Nantong, Jiangsu, China

² Department of Rehabilitation Medicine, Xuan Wu Hospital, Capital Medical University, Beijing, China

³ Department of Medical Imaging, Affiliated Hospital of Nantong University, Nantong, Jiangsu, China

⁴ Present address: Department of Rehabilitation Medicine, Nantong First People's Hospital, Nantong, China

(GCS) score < 13 in the first 24 h (Powers et al. 2019). In the United States of America, 1.4 million hospitalizations are due to traumatic brain injury (TBI) each year, and 80,000–90,000 patients will develop long-term disabilities (Centers for Disease et al., 2006). In addition, the lifetime risk of stroke is 25%, and strokes lead to ischemic or hemorrhagic brain injury (Collaborators et al. 2018). The mechanisms of brain injury include the damage to fragile tissues of the brain during acceleration/deceleration/shearing forces due to the irregular interior surface of the skull, cortical tissue injured by direct mechanical trauma, ischemia causing neuronal death, and hematomas and hemorrhage damaging the subcortical structures and leading to vasospasm and ischemia (Powers et al. 2019). Cognitive functions after SBI can be predicted by the duration of amnesia after trauma (Konigs et al. 2012) or by the extent of ischemia or hemorrhage (Powers et al. 2019). The overall mortality of SBI is 76% for patients with a GCS of 3 (National Institute for Health and Care Excellence (NICE), 2019).

In patients with subacute moderate brain injury, no significant computed tomography (CT) or magnetic resonance imaging (MRI) abnormalities can be observed, but frontal and occipital lobes hypoperfusion can be noted (Lin et al. 2016). In patients with severe TBI, MRI can reveal microbleeds (Moenninghoff et al. 2015). CT can also reveal brain hematoma, edema, subarachnoid hemorrhage, contusions, and midline shift (Schweitzer et al. 2019). Significantly reduced cerebral blood flow (CBF) and lymphatic flow, especially in the frontal and temporal lobes, have been reported in patients with chronic TBI assessed with single-photon emission CT (SPECT) (Raji et al. 2014).

Diffusion tensor imaging (DTI) is an advanced MRI technique that provides information about the connections within the brain and can reveal a pattern of disrupted connections (Douglas et al. 2015). DTI uses the detection of the diffusion of water molecules in tissues to observe nerve fibers' travel and structural integrity and then studies the fiber bundle connections in different functional brain regions. As the only non-invasive technique to track the movement of white matter fiber tracts in the brain in vivo, DTI has been applied in the research of brain injury related to cerebral ischemia, trauma, degeneration, and abnormal brain development, providing help for the discovery of disease and prognosis biomarkers for SBI patients (Douglas et al. 2015; Moura et al. 2019). Unlike clinical scores, DTI is not affected by sedatives or sleep and can be used to assess the white matter microstructure of patients with disturbances of consciousness (DoCs) in the resting state, avoiding data quality degradation caused by involuntary patient movement during data collection (Wu et al. 2018). Some researchers are trying to use DTI to identify different states of consciousness (such as unresponsive wakefulness

syndrome (UWS)/vegetative state (VS), minimally conscious state (MCS), etc.) of patients with DoCs caused by TBI or non-traumatic SBI, and analyze the relationship between the degree of injury and clinical prognosis (Jain et al. 2021; Yin et al. 2019).

Resting-state functional MRI (rs-fMRI) assesses the spontaneous, correlated fluctuations in the cerebral blood oxygenation level-dependent (BOLD) signal that occur between brain regions that are functionally related when the brain is not engaged in any specific task (Biswal et al. 2010). Therefore, rs-fMRI can be used to identify intrinsic neural networks and information about specific brain networks' connectivity and functionality (Seeley et al. 2007). Previous rs-fMRI studies in patients with SBI showed higher numbers of and stronger connections between medial prefrontal regions and other brain regions than controls (Iraji et al. 2015; Johnson et al. 2012; Mayer et al. 2015; Nathan et al. 2015).

Still, little data are available about the brain function and structure of patients with different levels of consciousness. Using patients with different levels of consciousness as the research subjects, this study sought to refine the classification of patients with prolonged disorders of consciousness (pDoCs) using a multimodal approach based on rs-fMRI and DTI technologies. This study might reveal the functional and structural changes in the brain function of patients with different levels of consciousness and the changes in white matter structural integrity. This multimodal research of pDoCs might unravel key brain regions and network mechanisms in patients with pDoCs. This study will also investigate the neural mechanisms of pDoCs during the dynamic follow-up of consciousness recovery of patients with pDoCs, according to the diagnostic criteria of pDoCs and validation using the coma recovery scale-revised (CRS-R) scale. In summary, this study aimed to explore the differences in the function and structural damage of key brain areas in patients with pDoCs with different levels of consciousness and the indicators for the prognosis of patients with pDoCs. The results could provide a new tool for determining the prognosis of patients with pDoCs.

Materials and Methods

Study Design and Patients

This prospective study included patients with SBI hospitalized in the department of rehabilitation medicine of the Affiliated Hospital of Nantong University. This study was approved by the Ethics Committee of the Affiliated Hospital of Nantong University (approval number: 2021-K017-01).

Written informed consent was obtained from the patients' legal guardians.

The inclusion criteria for the patients were (1) native Chinese speaker, (2) diagnosis of DoCs (including coma, UWS/VS, MCS, emergence from the minimally conscious state (eMCS), and locked-in syndrome (LIS) due to the first SBI (such as TBI, cerebrovascular diseases (CVD), HIE, etc.), (3) clinical diagnosis of coma, UWS/VS, MCS (including MCS+/-), eMCS, and LIS based on definitions and standardized diagnostic criteria recognized by international research and assessed by the CRS-R (Kondziella et al. 2020), (4) course of disease ≥ 28 days, (5) no history of vital organ injury or failure, stroke, cancer or brain tumor, neuropathy, brain surgery, or familial psychosis, (6) normal vision, hearing function, understanding ability, intelligence, and interpersonal skills before SBI, and (7) the patient and his family actively cooperated with treatment. The exclusion criteria were (1) metal implants such as electrical stimulators, arterial clamps, pacemakers, or hardware for skull repair, (2) damage to the brain structure was $> 25\%$ of the total brain volume, or (3) use of continuous intravenous sedative drugs (such as benzodiazepines or propofol) to induce artificial therapeutic coma.

MRI Examination and Image Processing

The patients were examined by MRI (Signa Excite 3.0T, GE Company, USA) with eight-channel standard head coil using a T2-weighted echo planar imaging (EPI) sequence: TR = 3000 ms, TE = 32 ms, 33 slices, voxel size = $4 \times 4 \times 4$ mm³, 128 volumes when they were admitted to the hospital. The patient lay supine on the examination table, with the head and neck between extension and flexion. Wearing noise-reducing headphones for MRI, the patient's head was fixed with bilateral sponge headrests to keep it still. An eight-channel standard head coil was used to scan the head from the base of the skull to the top of the skull. All patients underwent conventional serial cross-sectional imaging of T1WI, T2WI, T2 FLAIR, 3D-FSPGR sequence, BOLD scanning sequence, and DTI scanning sequence. The parameters of the different scanning sequences are shown in Supplementary Table S1.

MRI was preprocessed by local consistency processing method. The specific process is as follows: (1) DICOM format conversion: Convert the original data DICOM format to 3D NIFTI format. (2) Time correction: To reduce the influence caused by machine instability, the images of the first 12 time points of the scan were eliminated. (3) Head movement correction: pDoCs patients may produce a large number of artifacts due to excessive head movement, and the data with obvious head movement should be excluded. (4) Spatial normalization: Images were registered according to

the template of the Montreal Neurological Institute (MNI) standard brain space. (5) Spatial smoothing: Used to suppress noise and reduce interindividual variation introduced by residuals in gyral anatomy and function. The smoothing kernel of 6 mm was used in this study. Removal of linear drift: Correction of warming due to machine work or gradual adaptation of the subject, which may lead to changing distortions in the data image. (6) Filtering: It is generally believed that the characteristic frequency of the resting state is in the low frequency band, so we filtered the data at a low frequency (0.01 ~ 0.08 Hz).

After preprocessing the images, the preprocessed data was imported for regional homogeneity (ReHo) analysis, and the REST software was used to calculate Kendall's coefficient concordance (KCC) of 26 voxels for each voxel and domain to obtain the ReHo value of each voxel. The ReHo value of each voxel was normalized, and the ReHo value personal result file mReHo was obtained by dividing by the whole-brain average value. Finally, the mReHo result was spatially smoothed, and the smoothing kernel was 6 mm to obtain the smReHo file.

Diffusion-encoded images were acquired, using a single-shot echo-planar sequence (repetition time, 3000 ms; echo time, 56 ms; flip angle = 90° ; b-factor, 800 s mm²), from 15 different non-parallel directions with the baseline image being obtained without diffusion weighting ($b = 0$). Each volume consisted of 42 axial 3.0 mm slices with no gap (field of view, 230 mm \times 230 mm; acquisition matrix, 112×109 , reconstructed to 256×256). The FSL toolkit FLIRT was used to perform head movement and eddy current correction on DTI images. The toolkit BET v2.1 was used to remove non-brain tissues such as the scalp, skull, and background noise and obtain the whole-brain mask. The eigenvalues (λ_1 , λ_2 , and λ_3) and eigenvectors of the diffusion tensor were calculated using the Stejskal-Tanner equation (FDT v2.0). The anisotropy (fractional anisotropy, FA) value was defined as:

$$FA = \frac{\sqrt{(\lambda_1 - \lambda_2)^2 + (\lambda_1 - \lambda_3)^2 + (\lambda_2 - \lambda_3)^2}}{\sqrt{2(\lambda_1 + \lambda_2 + \lambda_3)}}$$

In order to calculate tract-based spatial statistics (TBSS), all FA images were aligned to a $1 \times 1 \times 1$ -mm standard space (affine nonlinear regression). The normalized images of each subject were merged to generate the FA average image, using standard image processing technology to skeletonize the average FA image to represent the main fiber bundle distribution of the subject. For FA value extraction, the standardized FA image was used to project onto the average skeleton template and extract from these templates. Generalized linear model modeling on the skeletonized images

was obtained by each subject to obtain the results of statistical analysis between groups based on each voxel.

Behavioral Assessments

All patients included in the study were evaluated using the GCS (Teasdale et al., 1974) and CRS-R (Kalmar et al., 2005) for at least five behavioral assessments within 1 week of admission to the hospital. The diagnosis of UWS/VS or MCS was based on the patient's highest CRS-R score. If serious complications (such as fever, respiratory/urinary tract infections, etc.) occurred, the diagnostic clinical evaluation was postponed until the patient's condition stabilized. In order to ensure the consistency of the study, the behavioral evaluations of the same patient in this study were all performed by the same rehabilitation physician or therapist.

Follow-up

All included patients with pDoCs were recorded at the time of admission and followed up at 1, 3, 6, and 12 months after entering the study. When the level of consciousness changed, the scales were evaluated, and the patient's consciousness changes were recorded. If the patient was still in the hospital during follow-up, an experienced rehabilitation physician or therapist conducted a bedside behavioral assessment of consciousness. If the patient had been discharged and transferred to another hospital during follow-up, telephone or video follow-up was conducted to assess the patient's state of consciousness every 6 months. If the patient died, the local doctor provided the patient's latest assessment results of the patient's level of consciousness. During follow-up, all physicians or therapists involved in the evaluation were ignorant of the grouping of the patients.

Outcomes

The primary outcomes were the state of consciousness assessed by the CRS-R scale at the end of follow-up and the state of functional disability classified by the Glasgow outcome scale (GOS) (Jennett et al., 1975), according to the clinical diagnosis of UWS/VS, MCS, and eMCS. Patients whose consciousness status changed to eMCS or fully regained consciousness (including LIS) during follow-up were classified as "conscious" (good outcome), while patients whose consciousness status was still UWS/VS or MCS (including MCS+/-) were classified as "unconscious" (poor outcome). Some patients regained consciousness but died of new disease events, and patients who died still unconscious were also included in the corresponding outcome categories.

Statistical Analysis

SPSS 22.0 (IBM, Armonk, NY, USA) was used for statistical analysis. Descriptive results were expressed as n (%), means \pm standard deviation, or medians (interquartile range (IQR)). The chi-square test or Fisher's exact test was used to test the categorical variables. The continuous variables were compared using the t-test or Mann-Whitney U-test. P -values < 0.05 were considered statistically significant.

The REST software was used to perform statistical analysis of smReHo between and within groups. The rest_sliceview software was used to view the anatomical parts corresponding to the Montreal Neurological Institute (MNI) coordinates. Brain regions with cluster > 228 voxels and $P < 0.05$ in each clump were related brain regions with statistically significant differences (the AlphaSim multiple correction was used for the results). The FA values of all subjects were statistically analyzed among the groups. First, the analysis of variance (ANOVA) was used, and then the post hoc test was performed in pairs to obtain the brain regions of the differences in the diffusion coefficients between the groups. The threshold value set for the statistical result was $P < 0.01$ or < 0.05 after multiple comparison corrections (family-wise error (fwe) correction).

Then, based on the preprocessed data, the region of interest (ROI) was selected for functional connection analysis. This study chose to extract the key brain areas of the internal consciousness network based on the automated anatomical labeling (AAL) atlas (bilateral thalamus, precuneus, anterior cingulate, and posterior cingulate) and key brain areas of the external consciousness network (bilateral superior frontal gyrus, and superior parietal gyrus), in conjunction with references. The following MNI coordinates were used as the center of the circle (left superior occipital gyrus, left triangle inferior frontal gyrus, left inferior temporal gyrus, cingulate gyrus, cerebellar parietal, middle temporal gyrus, medial frontal gyrus, insula, etc.) as ROI (Supplement Figure S1). The ReHo values of the above ROIs were extracted to compare groups based on the state of consciousness outcome grouping. The Pearson correlation analysis of different ROI and whole-brain ReHo values and behavioral scores was performed.

Results

Baseline Characteristics of the Patients

Thirty patients were enrolled, including eight with UWS/VS, eight with MCS, six with eMCS, and eight with LIS. Among them, 27 were males, and three were females. They were 13 to 79 (mean of 51.2 ± 15.3) years of age.

The etiology included 12 cases of TBI, 17 cases of CVD, and one case of HIE. The course of the disease was 35–403 days. The GCS score was 4–15, and the CRS-R score was 1–22 (Supplement Table S2).

According to the diagnostic criteria of pDoCs and the CRS-R score, at the end of follow-up, one UWS/VS patient entered MCS during the follow-up period, five MCS patients converted to eMCS or regained full consciousness, and all six eMCS patients recovered complete consciousness. Two MCS patients eventually died. Therefore, there were 19 patients in the conscious group and 11 in the unconscious group. There were no statistically significant differences in age and course of disease between the two groups ($P > 0.05$) (Table 1).

ReHo Analysis of Patients with Different Levels of Consciousness

Based on the results of the ReHo analysis, the significant activation area of the patients in the conscious group was in the right medial and lateral cingulate gyrus (voxel: 11065, MNI coordinates: 6, -12, 42, $t = 6.4305$). The significant activation area of the patients in the unconscious group was in the right lateral anterior cuneate (voxel: 4074, MNI coordinates: 15, -60, 48, $t = 8.5145$) and the left middle frontal gyrus (voxel: 412, MNI coordinates: -30, 45, 21, $t = 3.9453$) (Fig. 1 and Supplement Table S3).

Compared with the unconscious group, the peak brain area of ReHo was weakened in the unconscious group in the left basal nucleus (voxel: 55, MNI coordinates: -27, 0, 0, $t = -2.7932$), and the peak brain area of ReHo was enhanced in the left wedge anterior lobe (voxel: 90, MNI coordinates: -12, -60, 27, $t = 2.8303$) (Fig. 2 and Supplement Table S4).

DTI

The FA values of the patients were compared between the two groups to obtain the brain regions with differences in the diffusion coefficients. The threshold value of the tests

was set to $P < 0.01$. After multiple comparison corrections (FWE correction), the conscious group had higher amounts of white matter fiber tracts than the unconscious group in the corpus callosum, left cingulate gyrus, bilateral subfrontal tracts, bilateral anterior coronas, left corticospinal tract, and left posterior thalamus (Fig. 3).

Correlation Analysis between ReHo Values of Different ROIs and Behavioral Scores

Pearson correlation analysis showed a significant positive correlation between the ReHo value of the cerebellum and the GCS score ($r = 0.387$, $P = 0.038$) and between the ReHo value of the left temporal and the CRS-R score ($r = 0.394$, $P = 0.035$) (Tables 2 and 3).

Correlation Analysis of whole-brain ReHo Values and Behavioral Scores

The correlation analysis showed that the average ReHo value of the right middle temporal gyrus was negatively correlated with the GCS score ($r = -0.60$), the average ReHo values of the lower part of the cerebellum and the left lenticular putamen were positively correlated with the CRS-R score ($r = 0.53$ and $r = 0.52$), the average ReHo value of the left temporal pole was negatively correlated with the GOS score ($r = -0.62$), and the average ReHo values of the right posterior cerebellum and the left middle occipital gyrus were positively correlated with the GOS score ($r = 0.56$ and $r = 0.56$) (Fig. 4 and Supplement Table S5).

Discussion

Little data are available about the use of DTI and rs-fMRI in patients with pDoCs with different levels of consciousness. Therefore, this study aimed to explore the neural mechanisms with different levels of consciousness and the objective indicators for the prognosis of patients with pDoCs. The

Table 1 Patient baseline characteristics

	Total, $n = 30$	Conscious, $n = 19$	Unconscious, $n = 11$	P
Age (years), mean \pm SD	51.2 \pm 15.3	48.0 \pm 17.5	56.7 \pm 8.4	0.134
Male, n (%)	27 (90)	19 (100)	8 (72.7)	0.041*
Course of disease (days), mean \pm SD	71.5 (58.0, 123.3)	71.0 (61.0, 139.0)	79.0 (57.0, 115.0)	0.863
Cause n (%)				
TBI	12 (40)	3 (15.8)	9 (81.8)	0.003*
CVD	17 (56.7)	16 (84.2)	1 (9.1)	
HIE	1 (3.3)	0 (0)	1 (9.1)	
GCS on admission, median (IQR)	9 (7, 12)	11 (9, 12)	8 (5, 9)	0.001*
CRS-R on admission median (IQR)	10 (5.8, 19.5)	19 (10, 21)	5 (2, 8)	<0.001*

TBI: Traumatic brain injury; CVD: cerebrovascular disease; HIE: hypoxic-ischemic encephalopathy; GCS: Glasgow Coma Scale; CRS-R: Modified Coma Recovery Scale

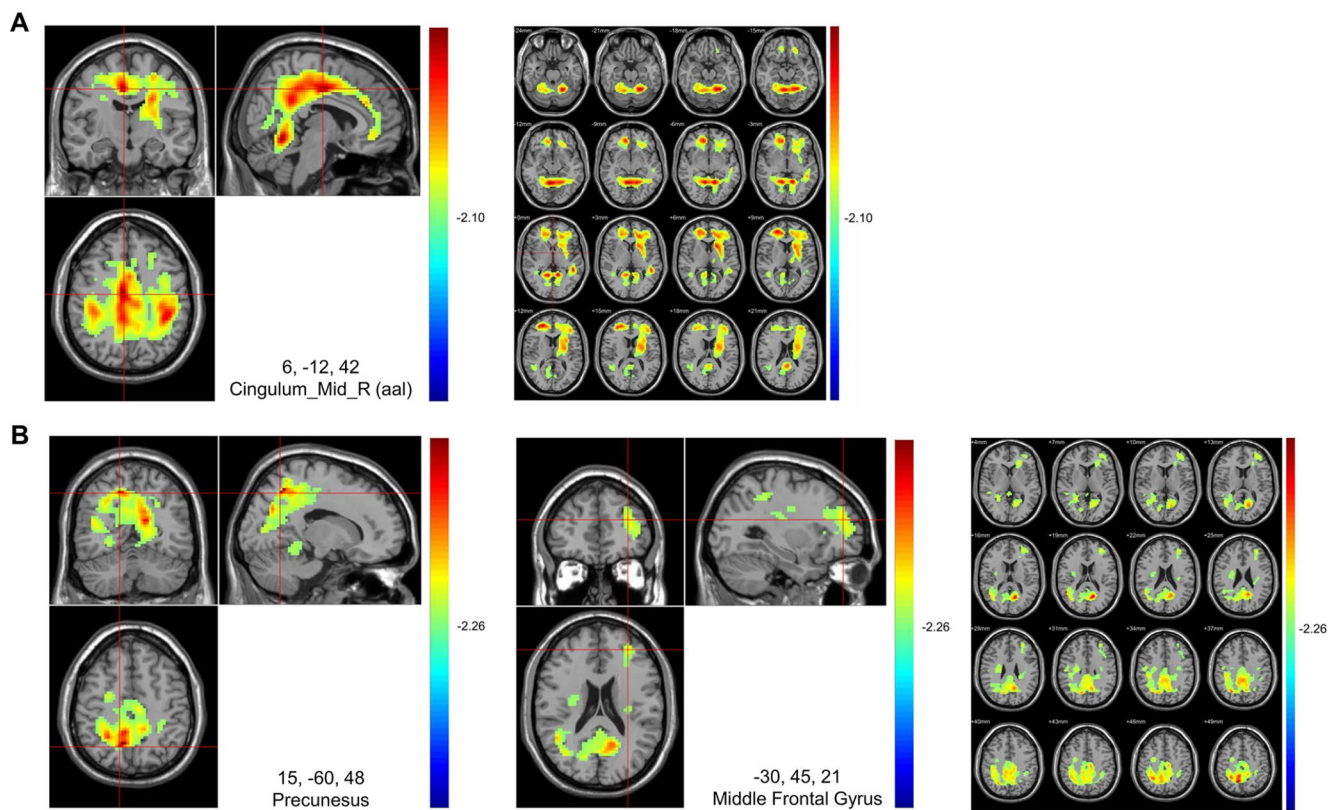


Fig. 1 rs-fMRI results of patients with different states of consciousness outcome. (A) Conscious group. (B) Unconscious group. All $P < 0.05$. Cluster size > 228

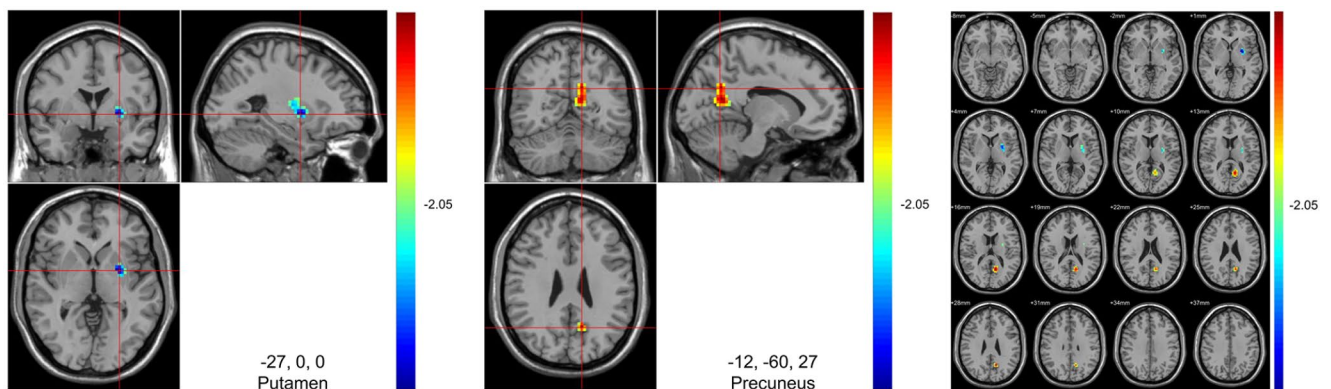


Fig. 2 Comparison of ReHo results between the unconscious and conscious groups of the outcome (warm color indicates high in the unconscious group; cold color indicates high in the conscious group). All $P < 0.05$. Cluster size > 50

left insula and cerebellum might be important for regaining consciousness. The brain function activity and structural remodeling of the key brain regions and the activation level of the cerebellum were correlated with clinical behaviors. This correlation has a potential application value for the prognosis prediction of pDoCs patients.

SBI has a variable outcome among different patients. In the present study, the patients with UWS/VS and MCS had different scale scores, consistent with the condition and diagnoses of the patients, and the characteristics of the patients

were similar between the two groups, which was similar to previous studies (Estraneo et al. 2016). In this study, one UWS/VS patient entered MCS during follow-up, five MCS patients converted to eMCS or regained full consciousness, and all six eMCS patients recovered complete consciousness. These results are supported by previous studies that showed better outcomes in patients with MCS (Seel et al. 2013; Steppacher et al. 2014), but the patient populations in the present study and previous studies are heterogeneous regarding the etiology of SBI and prognosis.

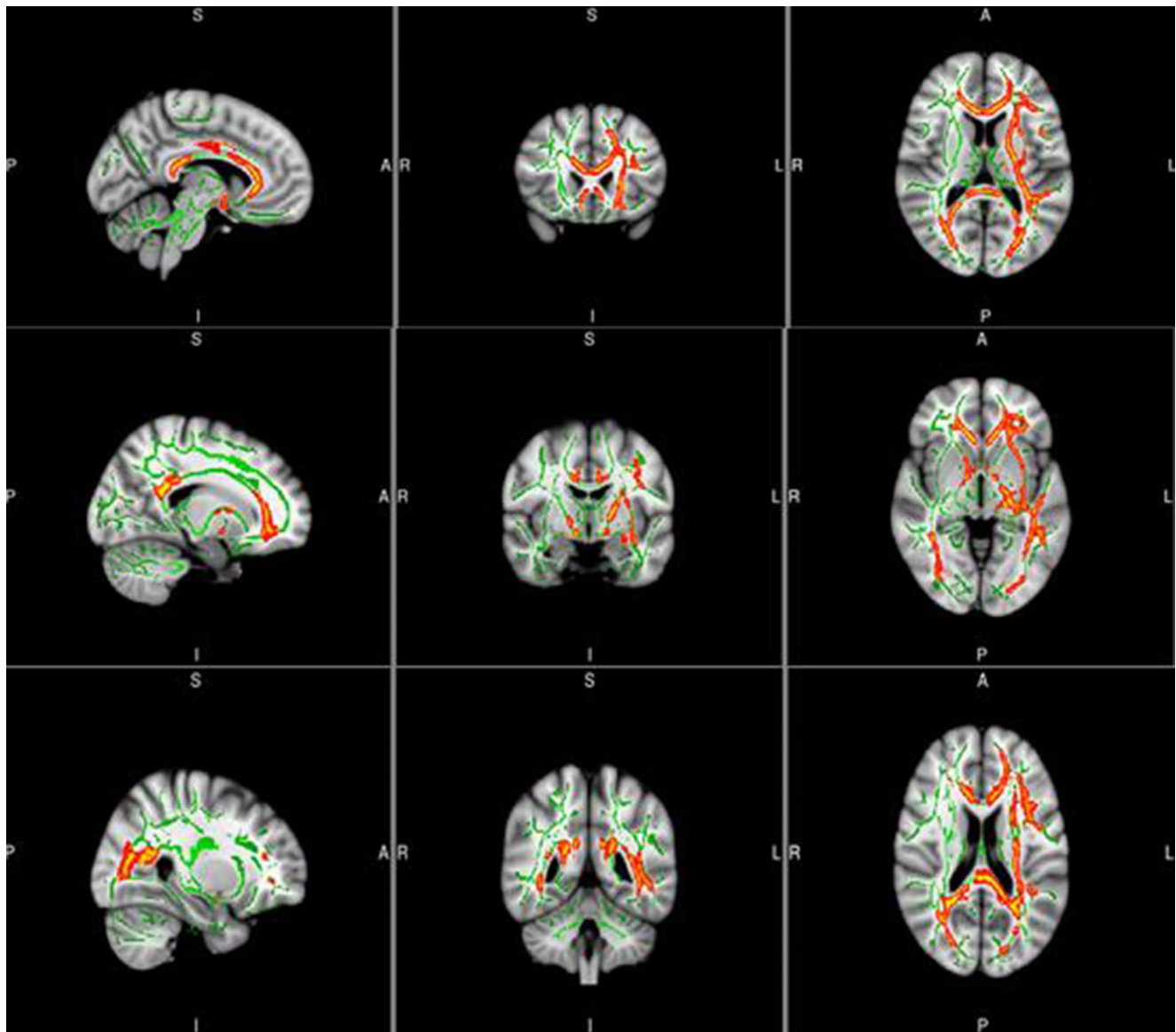


Fig. 3 FA statistical chart of the conscious vs. unconscious groups

This study examined the DTI and rs-fMRI characteristics of the patients according to whether they regained consciousness or not. Previous rs-fMRI studies in patients with SBI showed higher numbers of and stronger connections between medial prefrontal regions and other brain regions than controls (Iraji et al. 2015; Johnson et al. 2012; Mayer et al. 2015; Nathan et al. 2015), but these studies did not examine the results in terms of regaining consciousness or not. The present study showed that compared with the unconscious group, the left basal nucleus was activated in the conscious group, and DTI showed significant differences in white matter fiber bundles.

The default mode network (DMN) is the resting state network that received the most attention in the study of rs-fMRI patients in a coma. The DMN includes the posterior

cingulate/retrosplenial cortex, precuneus, medial prefrontal cortex, inferior parietal lobule (angular gyrus and supramarginal gyrus), and hippocampus (Buckner et al. 2008; Fransson et al., 2008). The DMN is compromised in SBI (Bonnelle et al. 2011, 2012; Hillary et al. 2011; Sharp et al. 2011; Soddu et al. 2012; Vanhaudenhuyse et al. 2010), and a longitudinal study showed that the restoration of the DMN connections correlates with recovery (Hillary et al. 2011). Changes in fMRI parameters have also been associated with consciousness recovery (Edlow et al. 2021). In addition, the severity of DMN impairment correlated with neurocognitive recovery (Bonnelle et al. 2011, 2012; Sharp et al. 2011). In addition, connectivity within the DMN correlated with white matter bundles by DTI (Bonnelle et al. 2011, 2012; Sharp et al. 2011).

Table 2 Details about region of interest

Label	Brain Region Name	Color or label
ROI1	Thalamus(77,78)	Red
ROI2	Precuneus(67,68)	Yellow
ROI3	Cingulum_Ant(31,32)	Green
ROI4	Cingulum_Post(35,36)	Sky blue
ROI5	Frontal_Sup(3,4)	purple
ROI6	Parietal_Sup(59,60)	Dark blue
ROI7	Occipital_Sup_L (aal)	-24 -75 24
ROI8	Frontal_Inf_Tri_L (aal)/ Inferior Frontal Gyrus	-45 39 9
ROI9	Temporal_Inf_L (aal)	-42 -51 -9
ROI10	Cingulate Gyrus	3-18 39
ROI11	Culmen	-15 -54 -12
ROI12	Cingulate Gyrus	-39 -51 45
ROI13	Middle Temporal Gyrus	39-66 21
ROI14	Medial Frontal Gyrus	-9 -15 72
ROI15	Insula	-36 9 -6
ROI16	Medial Frontal Gyrus	-9 -18 51
ROI17	Extra-Nuclear	-21 27 0
ROI18	Sub-Gyral	-12 -33 66
ROI19	Temporal Lobe	-54 -21 -6

In the present study, correlations were observed between the ReHo value of the cerebellum and GCS score, the ReHo value of the left temporal gyrus and the CRS-R score, the average ReHo value of the right middle temporal gyrus with the GCS score, the average ReHo values of the lower part of the cerebellum and the left lenticular putamen with the CRS-R score, the average value of the left temporal pole ReHo value with the GOS score, and the

average ReHo values of the right posterior cerebellum and the left middle occipital gyrus with the GOS score. These correlations globally are supported by Vanhaudenhuyse et al. (Vanhaudenhuyse et al. 2010), who showed that DMN connectivity correlated with the level of consciousness after traumatic SBI. Still, the exact correlations vary among studies because of the heterogeneity in SBI etiology and prognosis. Nevertheless, this study suggests that some rs-fMRI values could be associated with the outcomes of patients with pDoCs. Many patients with pDoCs are incorrectly classified (Schnakers et al. 2009), leading to major ethical issues and implications regarding prognosis, management, healthcare resources, and end-of-life decisions (Demertzi et al. 2014; Di Perri et al. 2016; Kondziella 2017, 2018). Therefore, this study suggests an examination that does not require the patient to be conscious or cooperative to predict the consciousness outcomes. The ongoing CONNECT-ME trial should shed additional light on the matter (Skibsted et al. 2018).

The rs-fMRI technique has limitations. The BOLD signal is only an indirect evaluation of neuronal activity and is affected by cerebral blood flow, the volume of blood, and the brain's oxygen consumption. The BOLD signal indicates changes in venous blood oxygenation, but no physiological units exist. In addition, artifacts are often encountered in rs-fMRI and can be caused by the behavioral state of the patient, hardware noise, respiration, and cardiac pulsation (Jo et al. 2010; Soddu et al. 2012). Therefore, care must be taken when comparing results among different studies. Still, rs-fMRI is the best fMRI option for patients who cannot

Table 3 Correlation analysis of ReHo value and the behavioral score of different ROIs (the results are corrected for multiple comparisons)

ROI	GCS		CRS		GOS	
	<i>r</i>	<i>P</i>	<i>r</i>	<i>P</i>	<i>r</i>	<i>P</i>
ROI1	0.184	0.339	0.155	0.421	-0.081	0.678
ROI2	-0.228	0.234	-0.256	0.180	-0.010	0.958
ROI3	0.160	0.408	0.075	0.701	0.006	0.977
ROI4	-0.098	0.612	-0.102	0.597	-0.150	0.437
ROI5	0.042	0.827	-0.045	0.817	0.164	0.395
ROI6	-0.090	0.643	-0.138	0.475	0.061	0.752
ROI7	-0.018	0.928	-0.048	0.805	0.123	0.525
ROI8	0.216	0.260	0.114	0.554	-0.009	0.963
ROI9	0.118	0.541	0.362	0.054	0.232	0.225
ROI10	-0.111	0.566	-0.277	0.146	-0.289	0.129
ROI11	0.387	0.038*	0.313	0.099	0.207	0.282
ROI12	-0.061	0.752	-0.017	0.932	0.193	0.317
ROI13	-0.232	0.225	-0.337	0.074	-0.229	0.232
ROI14	0.119	0.539	-0.006	0.976	0.315	0.097
ROI15	0.064	0.740	0.036	0.852	-0.160	0.407
ROI16	0.076	0.695	-0.159	0.409	-0.087	0.654
ROI17	0.092	0.634	-0.149	0.439	-0.055	0.775
ROI18	0.136	0.483	0.033	0.865	0.284	0.135
ROI19	0.260	0.173	0.394	0.035*	0.110	0.568

ROI: Region of interest; GCS: Glasgow Coma Scale; CRS-R: Modified Coma Recovery Scale; GOS: Glasgow Outcome Scale

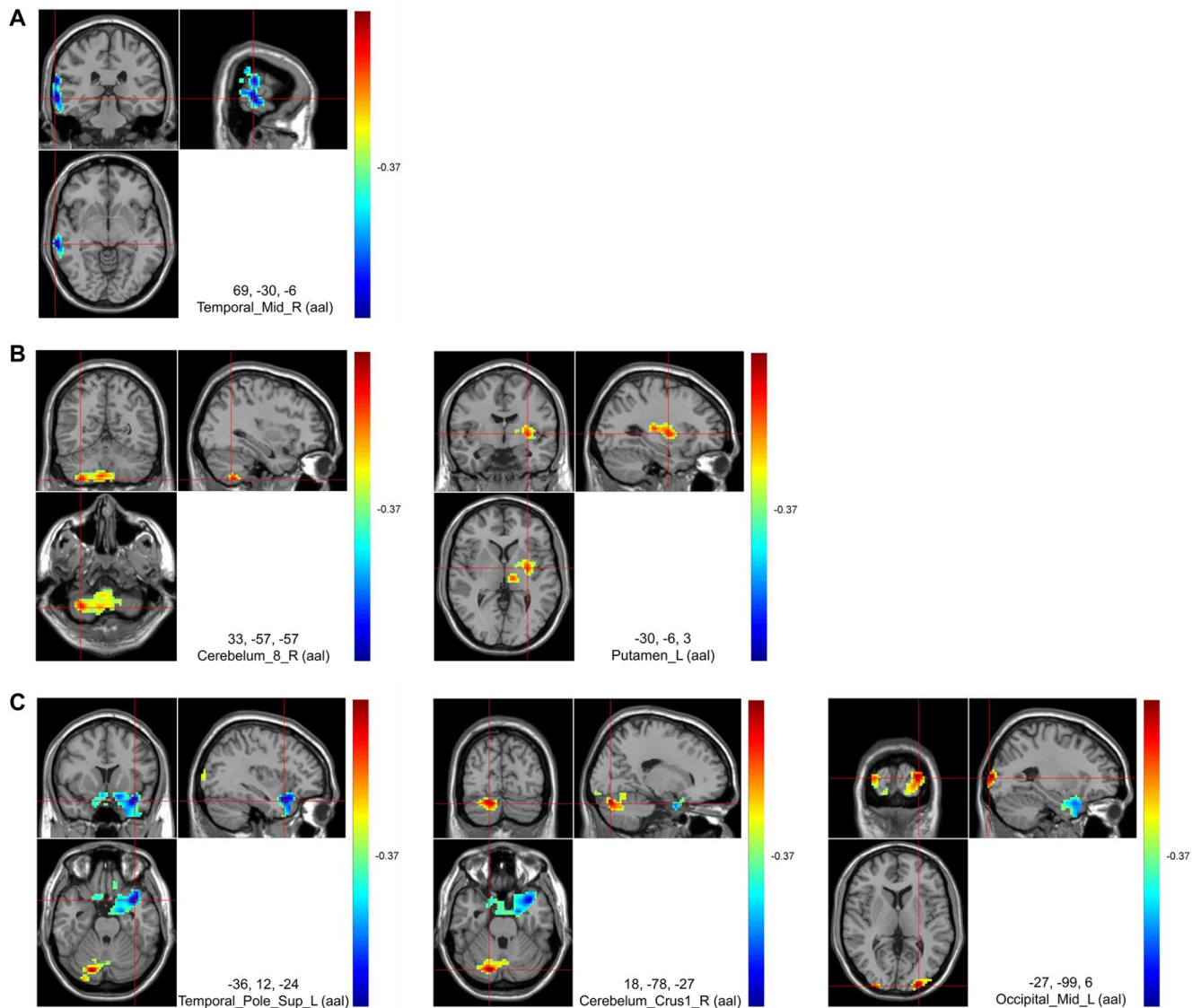


Fig. 4 Correlation results between behavioral scores and whole-brain ReHo values (warm colors indicate positive correlations; cold colors indicate negative correlations). (A) GCS score. (B) CRS score. (C) GOS score. All $P < 0.05$. Cluster size > 228

comply with task instructions (e.g., coma or unresponsive) (Edlow et al. 2013).

Furthermore, fMRI assesses the BOLD signal, while DTI assesses the diffusion of water along neuronal paths. Therefore, the two imaging modalities measure two different brain concepts that are complementary in evaluating patients with pDoCs. DTI can reveal whether neural pathways are physically disrupted, while fMRI evaluates whether there are functional changes in various brain areas. Still, the relationship between DTI and fMRI is complex. BOLD signals vary in direction and strength of association with white matter measurements, and these associations are affected by age (Bennett et al., 2013). A theory stipulates that higher white matter integrity will facilitate signals to grey matter regions, leading to increased blood flow (and

BOLD signals) in these regions. On the other hand, another theory stipulates that more efficient signals through white matter tracts will lead to more efficient interactions with grey matter and decreased metabolic demands by the grey matter, translating into decreased BOLD signals (Bennett and Rypma 2013). Compromised white matter integrity can produce a compensatory increased BOLD signal due to grey matter compensation (Park et al., 2009). Hence, given these discrepant theories, DTI and fMRI could be considered complementary for the prognosis of pDoCs.

Besides the rs-fMRI limitations, this study has limitations. First, the sample size of the study was relatively small, and there was no distinction between prognostic predictors such as different causes, disease courses, and lesion locations. Second, the results showed some prognostic predictors of

characteristic brain regions and white matter fiber tracts, but the mechanism cannot be fully explained, and some brain regions, for example, the classic PCC and precuneus ReHo, have different enhancements and weaknesses. Finally, the results were based on the group level, not the individual level. Future research also needs to expand further the sample size of the patients with different levels of consciousness, conduct long-term follow-up, and regularly check fMRI and DTI data to distinguish the relationship between the brain function and structural changes and prognosis of pDoCs patients with different causes, courses, and lesions. The method of level statistics has been further developed into multimodal neuroimaging technology to predict the prognosis of patients with pDoCs at the individual level.

Conclusions

In conclusion, although patients with pDoCs have strong predictors of poor prognosis, they may regain consciousness after a long recovery period. The accurate initial diagnosis and long-term regular follow-up of patients with pDoCs are essential for predicting results. The preservation of the dominant hemisphere, left insula, and cerebellum might be important targets for improving the patient's level of consciousness. Damage to the cerebral cortex impacts the pyramidal tract, and non-cerebral structures also play a key role in consciousness. The brain function activity and structural remodeling of the key brain regions of the DMN and the activation level of the cerebellum are correlated with clinical behaviors and have potential application value for the prognosis prediction of pDoCs patients. Hence, multimodal imaging using DTI and rs-fMRI could be used to determine the prognosis of patients with DoCs.

Supplementary Information The online version contains supplementary material available at <https://doi.org/10.1007/s10548-024-01087-7>.

Acknowledgements Not applicable.

Author Contributions WC: Conceptualization, Methodology, Software, Validation, Formal Analysis, Investigation, Resources, Data Curation, Writing Original Draft Preparation, Writing Review, Editing, Visualization, Funding Acquisition. YZ: Conceptualization, Methodology, Software, Validation, Investigation, Data Curation, Writing Review, Editing, Visualization, Funding Acquisition. AG: Supervision, Project Administration. XZ: Methodology, Software, Validation, Formal Analysis, Investigation, Resources, Visualization, Supervision. WS: Writing Review and Editing, Supervision, Project Administration, Funding Acquisition. All authors have read and agreed to the published version of the manuscript.

Funding This work was supported by The National Natural Science Foundation of China (NO: 81873723, 82102658) and the Nantong Municipal Social and People's Livelihood Science and Technology

Project (NO: MS12020018). The funders played no role in the design, conduct, or reporting of this study.

Data Availability The datasets generated during and/or analysed during the current study are available from the corresponding author on reasonable request.

Declarations

Ethics Approval This study was approved by the Ethics Committee of the Affiliated Hospital of Nantong University (approval number: 2021-K017-01).

Consent to Participate Written informed consent was obtained from the patients' legal guardians.

Consent to Publish Not applicable.

Conflict of interest The authors have no relevant financial or non-financial interests to disclose.

Competing Interests The authors declare no competing interests.

References

- Bennett IJ, Rypma B (2013) Advances in functional neuroanatomy: a review of combined DTI and fMRI studies in healthy younger and older adults. *Neurosci Biobehav Rev* 37:1201–1210. <https://doi.org/10.1016/j.neubiorev.2013.04.008>
- Biswal BB, Mennes M, Zuo XN, Gohel S, Kelly C, Smith SM, Beckmann CF, Adelstein JS, Buckner RL, Colcombe S, Dogonowski AM, Ernst M, Fair D, Hampson M, Hoptman MJ, Hyde JS, Kiviniemi VJ, Kotter R, Li SJ, Lin CP, Lowe MJ, Mackay C, Madden DJ, Madsen KH, Margulies DS, Mayberg HS, McMahon K, Monk CS, Mostofsky SH, Nagel BJ, Pekar JJ, Peltier SJ, Petersen SE, Riedl V, Rombouts SA, Rypma B, Schlaggar BL, Schmidt S, Seidler RD, Siegle GJ, Sorg C, Teng GJ, Veijola J, Villringer A, Walter M, Wang L, Weng XC, Whitfield-Gabrieli S, Williamson P, Windischberger C, Zang YF, Zhang HY, Castellanos FX, Milham MP (2010) Toward discovery science of human brain function. *Proc Natl Acad Sci U S A* 107:4734–4739. <https://doi.org/10.1073/pnas.0911855107>
- Bonnelle V, Leech R, Kinnunen KM, Ham TE, Beckmann CF, De Boissezon X, Greenwood RJ, Sharp DJ (2011) Default mode network connectivity predicts sustained attention deficits after traumatic brain injury. *J Neurosci* 31:13442–13451. <https://doi.org/10.1523/JNEUROSCI.1163-11.2011>
- Bonnelle V, Ham TE, Leech R, Kinnunen KM, Mehta MA, Greenwood RJ, Sharp DJ (2012) Salience network integrity predicts default mode network function after traumatic brain injury. *Proc Natl Acad Sci U S A* 109:4690–4695. <https://doi.org/10.1073/pnas.1113455109>
- Buckner RL, Andrews-Hanna JR, Schacter DL (2008) The brain's default network: anatomy, function, and relevance to disease. *Ann N Y Acad Sci* 1124:1–38. <https://doi.org/10.1196/annals.1440.011>
- Centers for Disease C, Prevention (2006) Incidence rates of hospitalization related to traumatic brain injury—12 states, 2002. *MMWR Morb Mortal Wkly Rep* 55:201–204
- Collaborators GBDLRS, Feigin VL, Nguyen G, Cercy K, Johnson CO, Alam T, Parmar PG, Abajobir AA, Abate KH, Abd-Allah F, Abejie AN, Abyu GY, Ademi Z, Agarwal G, Ahmed MB, Akinyemi RO, Al-Raddadi R, Aminde LN, Amlic-Lefond C,

- Ansari H, Asayesh H, Asgedom SW, Atey TM, Ayele HT, Banach M, Banerjee A, Barac A, Barker-Collo SL, Barnighausen T, Barregard L, Basu S, Bedi N, Behzadifar M, Bejot Y, Bennett DA, Bensenor IM, Berhe DF, Boneya DJ, Brainin M, Campos-Nonato IR, Caso V, Castaneda-Orjuela CA, Rivas JC, Catala-Lopez F, Christensen H, Criqui MH, Damasceno A, Dandona L, Dandona R, Davletov K, de Courten B, deVeber G, Dokova K, Edessa D, Endres M, Faraon EJA, Farvid MS, Fischer F, Foreman K, Forouzanfar MH, Gall SL, Gebrehiwot TT, Geleijnse JM, Gillum RF, Giroud M, Goulart AC, Gupta R, Gupta R, Hachinski V, Hamadeh RR, Hankey GJ, Hareri HA, Havmoeller R, Hay SI, Hegazy MI, Hibstu DT, James SL, Jeemon P, John D, Jonas JB, Jozwiak J, Kalani R, Kandel A, Kasaieian A, Kengne AP, Khader YS, Khan AR, Khang YH, Khubchandani J, Kim D, Kim YJ, Kivimaki M, Kokubo Y, Kolte D, Kopec JA, Kosen S, Kravchenko M, Krishnamurthi R, Kumar GA, Lafranconi A, Lavados PM, Legesse Y, Li Y, Liang X, Lo WD, Lorkowski S, Lotufo PA, Loy CT, Mackay MT, Abd El Razek HM, Mahdavi M, Majeed A, Malekzadeh R, Malta DC, Mamun AA, Mantovani LG, Martins SCO, Mate KK, Mazidi M, Mehata S, Meier T, Melaku YA, Mendoza W, Mensah GA, Meretoja A, Mezgebe HB, Miazgowski T, Miller TR, Ibrahim NM, Mohammed S, Mokdad AH, Moosazadeh M, Moran AE, Musa KI, Negoi RI, Nguyen M, Nguyen QL, Nguyen TH, Tran TT, Nguyen TT, Anggraini Ningrum DN, Norrving B, Noubiap JJ, O'Donnell MJ, Olagunju AT, Onuma OK, Owolabi MO, Parsaieian M, Patton GC, Piradov M, Pletcher MA, Pourmalek F, Prakash V, Qorbani M, Rahman M, Rahman MA, Rai RK, Ranta A, Rawaf D, Rawaf S, Renzaho AM, Robinson SR, Sahathevan R, Sahebkar A, Salomon JA, Santalucia P, Santos IS, Sartorius B, Schutte AE, Sepanlou SG, Shafieesabet A, Shaikh MA, Shamsizadeh M, Sheth KN, Sisay M, Shin MJ, Shiue I, Silva DAS, Sobngwi E, Soljak M, Sorensen RJD, Sposato LA, Stranges S, Suliankatchi RA, Tabares-Seisdedos R, Tanne D, Nguyen CT, Thakur JS, Thrift AG, Tirschwell DL, Topor-Madry R, Tran BX, Nguyen LT, Truelsen T, Tsilimparis N, Tyrovolas S, Ukwaja KN, Uthman OA, Varakin Y, Vasankari T, Venketasubramanian N, Vlassov VV, Wang W, Werdecker A, Wolfe CDA, Xu G, Yano Y, Yonemoto N, Yu C, Zaidi Z, El Sayed Zaki M, Zhou M, Ziaeian B, Zipkin B, Vos T, Naghavi M, Murray CJL, Roth GA (2018) Global, Regional, and Country-Specific Lifetime Risks of Stroke, 1990 and 2016. *N Engl J Med* 379: 2429–2437. <https://doi.org/10.1056/NEJMoa1804492>
- Demertzi A, Jox RJ, Racine E, Laureys S (2014) A European survey on attitudes towards pain and end-of-life issues in locked-in syndrome. *Brain Inj* 28:1209–1215. <https://doi.org/10.3109/02699052.2014.920526>
- Di Perri C, Bahri MA, Amico E, Thibaut A, Heine L, Antonopoulos G, Charland-Verville V, Wannez S, Gomez F, Hustinx R, Tshibanda L, Demertzi A, Soddu A, Laureys S (2016) Neural correlates of consciousness in patients who have emerged from a minimally conscious state: a cross-sectional multimodal imaging study. *Lancet Neurol* 15:830–842. [https://doi.org/10.1016/S1474-4422\(16\)00111-3](https://doi.org/10.1016/S1474-4422(16)00111-3)
- Douglas DB, Iv M, Douglas PK, Anderson A, Vos SB, Bammer R, Zeineh M, Wintermark M (2015) Diffusion Tensor Imaging of TBI: potentials and challenges. *Top Magn Reson Imaging* 24:241–251. <https://doi.org/10.1097/RMR.0000000000000062>
- Edlow BL, Giacino JT, Wu O (2013) Functional MRI and outcome in traumatic coma. *Curr Neurol Neurosci Rep* 13:375. <https://doi.org/10.1007/s11910-013-0375-y>
- Edlow BL, Claassen J, Schiff ND, Greer DM (2021) Recovery from disorders of consciousness: mechanisms, prognosis and emerging therapies. *Nat Rev Neurol* 17:135–156. <https://doi.org/10.1038/s41582-020-00428-x>
- Estraneo A, Loreto V, Guarino I, Boemia V, Paone G, Moretta P, Trojano L (2016) Standard EEG in diagnostic process of prolonged disorders of consciousness. *Clin Neurophysiol* 127:2379–2385. <https://doi.org/10.1016/j.clinph.2016.03.021>
- Fransson P, Marrelec G (2008) The precuneus/posterior cingulate cortex plays a pivotal role in the default mode network: evidence from a partial correlation network analysis. *NeuroImage* 42:1178–1184. <https://doi.org/10.1016/j.neuroimage.2008.05.059>
- Hillary FG, Slocumb J, Hills EC, Fitzpatrick NM, Medaglia JD, Wang J, Good DC, Wylie GR (2011) Changes in resting connectivity during recovery from severe traumatic brain injury. *Int J Psychophysiol* 82:115–123. <https://doi.org/10.1016/j.ijpsycho.2011.03.011>
- Iraji A, Benson RR, Welch RD, O'Neil BJ, Woodard JL, Ayaz SI, Kulek A, Mika V, Medado P, Soltanian-Zadeh H, Liu T, Haacke EM, Kou Z (2015) Resting state functional connectivity in mild traumatic brain injury at the Acute Stage: independent component and seed-based analyses. *J Neurotrauma* 32:1031–1045. <https://doi.org/10.1089/neu.2014.3610>
- Jain B, Das AK, Agrawal M, Babal R, Purohit DK (2021) Implications of DTI in mild traumatic brain injury for detecting neurological recovery and predicting long-term behavioural outcome in paediatric and young population—a systematic review. *Childs Nerv Syst* 37:2475–2486. <https://doi.org/10.1007/s00381-021-05240-6>
- Jennett B, Bond M (1975) Assessment of outcome after severe brain damage. *Lancet* 1:480–484. [https://doi.org/10.1016/S0140-6736\(75\)92830-5](https://doi.org/10.1016/S0140-6736(75)92830-5)
- Jo HJ, Saad ZS, Simmons WK, Milbury LA, Cox RW (2010) Mapping sources of correlation in resting state fMRI, with artifact detection and removal. *NeuroImage* 52:571–582. <https://doi.org/10.1016/j.neuroimage.2010.04.246>
- Johnson B, Zhang K, Gay M, Horovitz S, Hallett M, Sebastianelli W, Slobounov S (2012) Alteration of brain default network in subacute phase of injury in concussed individuals: resting-state fMRI study. *NeuroImage* 59:511–518. <https://doi.org/10.1016/j.neuroimage.2011.07.081>
- Kalmar K, Giacino JT (2005) The JFK Coma Recovery scale—revised. *Neuropsychol Rehabil* 15:454–460. <https://doi.org/10.1080/09602010443000425>
- Kondziella D (2017) Roald Dahl and the complete locked-in syndrome: Cold dead body, living brain. *J Neurol Sci* 379:276–278. <https://doi.org/10.1016/j.jns.2017.06.033>
- Kondziella D (2018) Functional neuroimaging in disorders of consciousness: raising awareness for those with decreased awareness. *Neuroscience* 382:125–126. <https://doi.org/10.1016/j.neuroscience.2018.03.046>
- Kondziella D, Bender A, Diserens K, van Erp W, Estraneo A, Formisano R, Laureys S, Naccache L, Ozturk S, Rohaut B, Sitt JD, Stender J, Tiainen M, Rossetti AO, Gosseries O, Chatelle C, Ean Panel on Coma DoC (2020) European Academy of Neurology guideline on the diagnosis of coma and other disorders of consciousness. *Eur J Neurol* 27:741–756. <https://doi.org/10.1111/en.14151>
- Konigs M, de Kieviet JF, Oosterlaan J (2012) Post-traumatic amnesia predicts intelligence impairment following traumatic brain injury: a meta-analysis. *J Neurol Neurosurg Psychiatry* 83:1048–1055. <https://doi.org/10.1136/jnnp-2012-302635>
- Lin CM, Tseng YC, Hsu HL, Chen CJ, Chen DY, Yan FX, Chiu WT (2016) Arterial spin labeling perfusion study in the patients with subacute mild traumatic brain injury. *PLoS ONE* 11:e0149109. <https://doi.org/10.1371/journal.pone.0149109>
- Mayer AR, Ling JM, Allen EA, Klimaj SD, Yeo RA, Hanlon FM (2015) Static and dynamic intrinsic connectivity following mild traumatic brain injury. *J Neurotrauma* 32:1046–1055. <https://doi.org/10.1089/neu.2014.3542>
- Moenninghoff C, Kraff O, Maderwald S, Umutlu L, Theysohn JM, Ringelstein A, Wrede KH, Deuschl C, Altmepfen J, Ladd ME, Forsting M, Quick HH, Schlamann M (2015) Diffuse axonal

- injury at ultra-high field MRI. *PLoS ONE* 10:e0122329. <https://doi.org/10.1371/journal.pone.0122329>
- Moura LM, Luccas R, de Paiva JPQ, Amaro E Jr., Leemans A, Leite CDC, Otaduy MCG, Conforto AB (2019) Diffusion Tensor Imaging biomarkers to Predict Motor outcomes in Stroke: a narrative review. *Front Neurol* 10:445. <https://doi.org/10.3389/fneur.2019.00445>
- Nathan DE, Oakes TR, Yeh PH, French LM, Harper JF, Liu W, Wolfowitz RD, Wang BQ, Graner JL, Riedy G (2015) Exploring variations in functional connectivity of the resting state default mode network in mild traumatic brain injury. *Brain Connect* 5:102–114. <https://doi.org/10.1089/brain.2014.0273>
- National Institute for Health and Care Excellence (NICE) (2019) Head injury: assessment and early management (CG176). National Institute for Health and Care Excellence, London
- Park DC, Reuter-Lorenz P (2009) The adaptive brain: aging and neurocognitive scaffolding. *Annu Rev Psychol* 60:173–196. <https://doi.org/10.1146/annurev.psych.59.103006.093656>
- Powers WJ, Rabinstein AA, Ackerson T, Adeoye OM, Bambakidis NC, Becker K, Biller J, Brown M, Demaerschalk BM, Hoh B, Jauch EC, Kidwell CS, Leslie-Mazwi TM, Ovbiagele B, Scott PA, Sheth KN, Southerland AM, Summers DV, Tirschwell DL (2019) Guidelines for the early management of patients with Acute ischemic stroke: 2019 update to the 2018 guidelines for the early management of Acute ischemic stroke: a Guideline for Healthcare professionals from the American Heart Association/American Stroke Association. *Stroke* 50:e344–e418. <https://doi.org/10.1161/STR.0000000000000211>
- Raji CA, Tarzwell R, Pavel D, Schneider H, Uszler M, Thornton J, van Lierop M, Cohen P, Amen DG, Henderson T (2014) Clinical utility of SPECT neuroimaging in the diagnosis and treatment of traumatic brain injury: a systematic review. *PLoS ONE* 9:e91088. <https://doi.org/10.1371/journal.pone.0091088>
- Schnakers C, Vanhaudenhuyse A, Giacino J, Ventura M, Boly M, Majerus S, Moonen G, Laureys S (2009) Diagnostic accuracy of the vegetative and minimally conscious state: clinical consensus versus standardized neurobehavioral assessment. *BMC Neurol* 9:35. <https://doi.org/10.1186/1471-2377-9-35>
- Schweitzer AD, Niogi SN, Whitlow CT, Tsiouris AJ (2019) Traumatic Brain Injury: imaging patterns and complications. *Radiographics* 39:1571–1595. <https://doi.org/10.1148/rg.2019190076>
- Seel RT, Douglas J, Dennison AC, Heaner S, Farris K, Rogers C (2013) Specialized early treatment for persons with disorders of consciousness: program components and outcomes. *Arch Phys Med Rehabil* 94:1908–1923. <https://doi.org/10.1016/j.apmr.2012.11.052>
- Seeley WW, Menon V, Schatzberg AF, Keller J, Glover GH, Kenna H, Reiss AL, Greicius MD (2007) Dissociable intrinsic connectivity networks for salience processing and executive control. *J Neurosci* 27:2349–2356. <https://doi.org/10.1523/JNEUROSCI.5587-06.2007>
- Sharp DJ, Beckmann CF, Greenwood R, Kinnunen KM, Bonnelle V, De Boissezon X, Powell JH, Counsell SJ, Patel MC, Leech R (2011) Default mode network functional and structural connectivity after traumatic brain injury. *Brain* 134:2233–2247. <https://doi.org/10.1093/brain/awr175>
- Skibsted AP, Amiri M, Fisher PM, Sidaros A, Hribljan MC, Larsen VA, Hojgaard JLS, Nikolic M, Hauerberg J, Fabricius ME, Knudsen GM, Moller K, Kondziella D (2018) Consciousness in Neurocritical Care Cohort Study using fMRI and EEG (CONNECT-ME): protocol for a longitudinal prospective study and a Tertiary Clinical Care Service. *Front Neurol* 9:1012. <https://doi.org/10.3389/fneur.2018.01012>
- Soddu A, Vanhaudenhuyse A, Bahri MA, Bruno MA, Boly M, Demertzi A, Tshibanda JF, Phillips C, Stanziano M, Ovadia-Caro S, Nir Y, Maquet P, Papa M, Malach R, Laureys S, Noirhomme Q (2012) Identifying the default-mode component in spatial IC analyses of patients with disorders of consciousness. *Hum Brain Mapp* 33:778–796. <https://doi.org/10.1002/hbm.21249>
- Stepbacher I, Kaps M, Kissler J (2014) Will time heal? A long-term follow-up of severe disorders of consciousness. *Ann Clin Transl Neurol* 1:401–408. <https://doi.org/10.1002/acn3.63>
- Teasdale G, Jennett B (1974) Assessment of coma and impaired consciousness. A practical scale. *Lancet* 2:81–84. [https://doi.org/10.1016/s0140-6736\(74\)91639-0](https://doi.org/10.1016/s0140-6736(74)91639-0)
- Vanhaudenhuyse A, Noirhomme Q, Tshibanda LJ, Bruno MA, Boveroux P, Schnakers C, Soddu A, Perlberg V, Ledoux D, Brichant JF, Moonen G, Maquet P, Greicius MD, Laureys S, Boly M (2010) Default network connectivity reflects the level of consciousness in non-communicative brain-damaged patients. *Brain* 133:161–171. <https://doi.org/10.1093/brain/awp313>
- Wu X, Zhang J, Cui Z, Tang W, Shao C, Hu J, Zhu J, Zhao Y, Lu L, Chen G, Northoff G, Gong G, Mao Y, He Y (2018) White Matter deficits underlying the impaired consciousness level in patients with disorders of consciousness. *Neurosci Bull* 34:668–678. <https://doi.org/10.1007/s12264-018-0253-3>
- Yin B, Li DD, Huang H, Gu CH, Bai GH, Hu LX, Zhuang JF, Zhang M (2019) Longitudinal changes in Diffusion Tensor Imaging following mild traumatic brain Injury and correlation with outcome. *Front Neural Circuits* 13:28. <https://doi.org/10.3389/fncir.2019.00028>

Publisher's Note Springer Nature remains neutral with regard to jurisdictional claims in published maps and institutional affiliations.

Springer Nature or its licensor (e.g. a society or other partner) holds exclusive rights to this article under a publishing agreement with the author(s) or other rightsholder(s); author self-archiving of the accepted manuscript version of this article is solely governed by the terms of such publishing agreement and applicable law.